[A9] Detection of melt ponds on sea ice in the Chukchi Sea in summer season using TerraSAR-X dual-polarization data

Miae Kim[1], Hyangsun Han[2], Jungho Im[1], Seongmun Sim[1]
[1] School of Urban and Environmental Engineering, UNIST, Ulsan, South Korea
[2] Korea Polar Research Institute, Incheon, South Korea

Abstract

Melt ponds are common features of the summertime Arctic sea ice, absorbing incoming solar radiation and affecting the melting rate of sea ice. The accurate monitoring of melt ponds is needed to better understand the sea ice-climate interaction. In this study, melt pond retrieval models were developed with TerraSAR-X dual-polarization data using machine learning approaches—decision trees (DT) and random forest (RF). To construct a reference dataset, three classes (melt ponds, sea ice, and open water) were delineated from airborne SAR images of 0.3 m resolution. A total of 8 polarimetric parameters were derived from the TerraSAR-X data to be used as input variables for the machine learning models. As a result, melt ponds could not be distinguished from open water with only the polarimetric parameters due to similar polarimetric signatures to open water. Thus, texture features (mean and STD) of the polarimetric parameters based on a 15×15 pixel window were added to the input variables. **Both DT and RF models with the polarimetric parameters and their texture features produced much improved performance for the retrieval of melt ponds. The melt pond fraction and sea ice concentration retrieved from the RF-derived melt pond map showed relatively low RMSDs, compared to those from the reference melt pond maps.** This indicates that the accurate monitoring of melt pond fraction at a local scale can be performed using high-resolution dual-pol SAR data. This research is under review at *Remote Sensing* journal.

Data and Methods

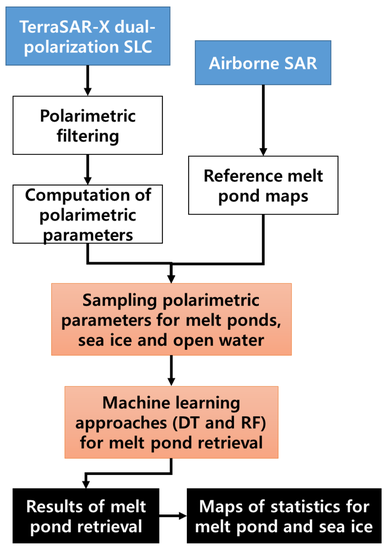

Figure 1. Processing flow of melt pond retrieval.

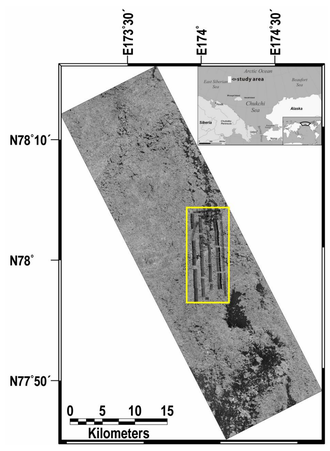

Figure 2. Airborne SAR images overlaid on a TerraSAR-X amplitude (HH-polarization) image of the study area.

Construction of reference dataset

In order to construct a reference dataset to classify open water, sea ice, and melt pond, the objects of each class were delineated using image processing software, ENVI. First, water and ice were classified from the object extraction procedure. The water objects within the ice were defined as melt ponds. In some airborne SAR images, open water within interconnected ice floes was misclassified as a melt pond. To reduce the misclassification, the melt pond objects with an area larger than 700 m² were considered to be open water [1]. The classification result of the airborne SAR images were used as a reference dataset for the classification of the TerraSAR-X data.

Polarimetric parameters used as model input variables

A total of 8 polarimetric parameters derived from the TerraSAR-X dual-polarization data are including HH and VV backscattering coefficients, co-polarization ratio, co-polarization phase difference, co-polarization correlation coefficient, alpha angle, entropy, and anisotropy.

Statistics for melt ponds

The statistics for melt ponds were computed from the individual airborne SAR images including as below.

1) Melt pond fraction (F_p): the percentage of total ice area covered by melt ponds $[A_p^* / (A_i^{**} + A_p)]$

2) Number density of ponds (N_d): the number of melt ponds divided by the area of sea ice including melt ponds ($A_i + A_p$) with units of km^{-2}

3) Mean pond size (S_p)

4) Sea ice concentration: the fraction of sea ice including melt pond areas within the image

$^*A_p$: the fraction of melt ponds within an airborne SAR image

$^{**}A_i$: the fraction of sea ice excluding melt pond areas within the image

Machine learning approaches

Binary Decision Trees

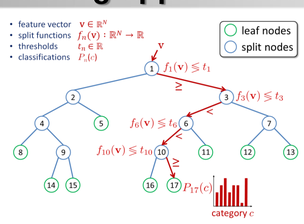

Random Forest
Forest is ensemble of several decision trees

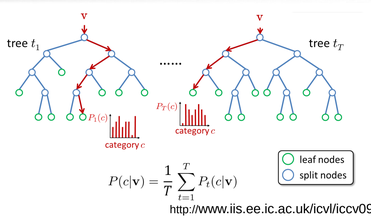

http://www.iis.ee.ic.ac.uk/icvl/iccv09_tutorial.html

Results and Discussion

Polarimetric texture signatures

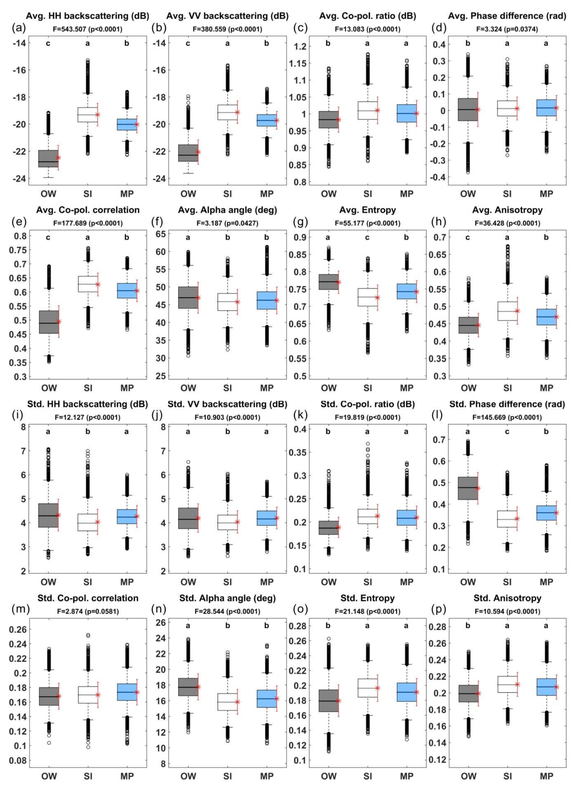

Figure 3. Boxplots of the texture features of the polarimetric parameters used for melt pond retrieval.

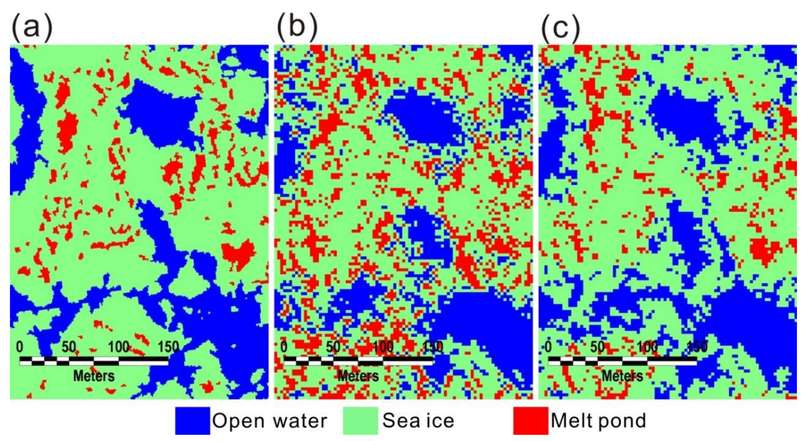

Figure 4. Comparison between (a) the airborne SAR- and machine learning results-based melt pond maps: (b) the DT model and (c) the RF model.

Performance of melt pond detection model

Table 1. Accuracy assessment for DT model with the polarimetric parameters and their texture features.

Classified as \ Reference	Open water	Sea ice	Melt pond	Sum	User's accuracy
Open water	2333	14	210	2557	91.24%
Sea ice	15	2175	434	2624	82.89%
Melt pond	129	288	1833	2250	81.47%
Sum	2477	2477	2477	7431	
Producer's accuracy	94.19%	87.81%	74.0%		
Overall accuracy	85.33%				
Kappa coefficient	78.0%				

Table 2. Accuracy assessment for RF model with the polarimetric parameters and their texture features.

Classified as \ Reference	Open water	Sea Ice	Melt pond	Sum	User's accuracy
Open water	2366	7	125	2498	94.72%
Sea ice	5	2280	304	2589	88.06%
Melt pond	106	190	2048	2344	87.37%
Sum	2477	2477	2477	7431	
Producer's accuracy	95.52%	92.04%	82.68%		
Overall accuracy	90.08%				
Kappa coefficient	85.12%				

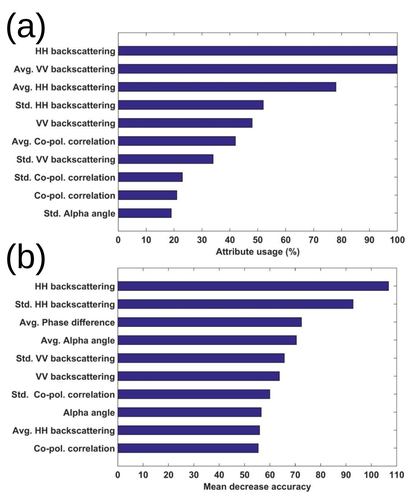

Figure 5. Relative variable importance of (a) the DT and (b) RF model.

Retrieved melt pond statistics

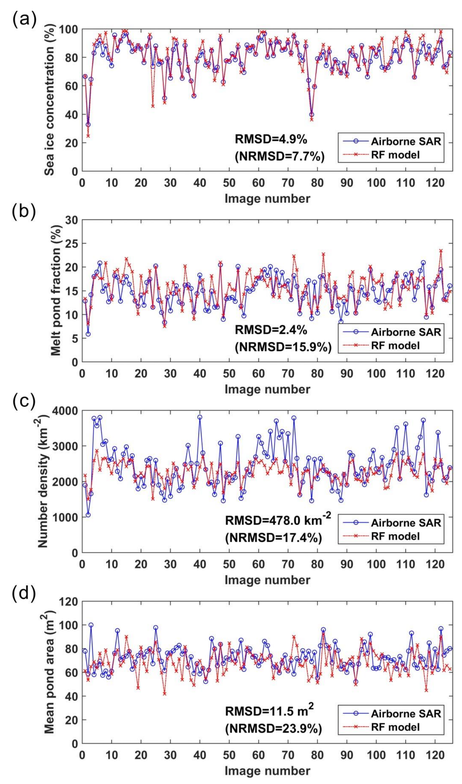

Figure 6. Comparison between the airborne SAR- and the RF model-derived statistics for melt pond and sea ice.

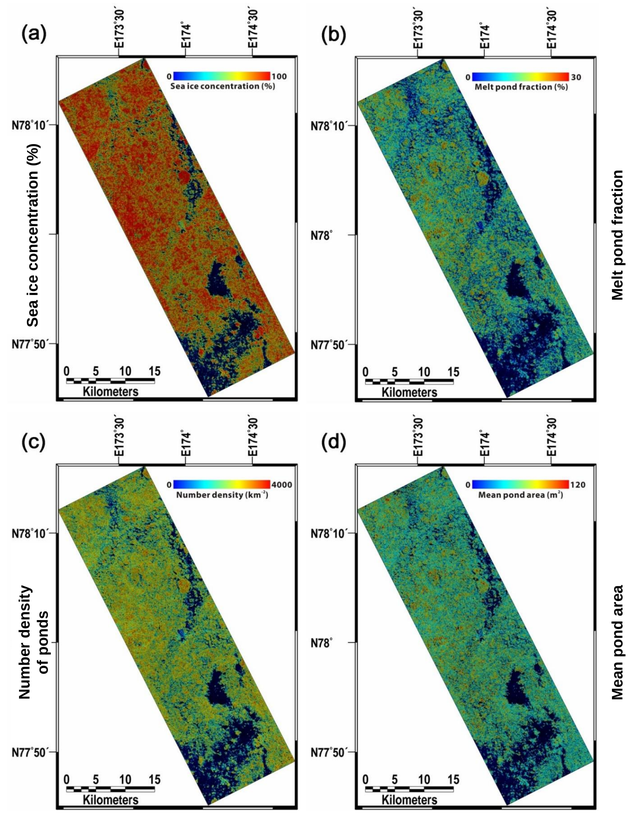

Figure 7. Maps of the statistics for melt pond and sea ice generated from the RF model-derived melt pond map.

Reference

[1] Kim, D.-J.; Hwang, B.; Chung, K.H.; Lee, S.H.; Jung, H.S.; Moon, W.M. Melt pond mapping with high-resolution SAR: The first view. *Proc. IEEE* **2013**, *101*, 748–758.